

Microstructure and Wear of Cathodic Arc Physical Vapour Deposited on TiAlN, TiCrN and n-TiAlN/ α -Si₃N₄ Films

Manish Roy^{*,#}, S. Saha, and K. Valleti[@]

[#]DRDO-Defence Metallurgical Research Laboratory, Hyderabad - 500 058, India

[@]International Advanced Research Center for Powder Metallurgy and New Materials, Hyderabad - 500 005, India

^{*}E-mail: manish@dmrl.drdo.in

ABSTRACT

Present study examined the microstructural features, hardness and wear performance of TiAlN, TiCrN and n-TiAlN/ α -Si₃N₄ coatings deposited by cathodic arc physical vapour deposition (CA-PVD) technique on M-50 steel keeping in mind a possible application of hybrid bearings in next generation aero-engine. Microstructural features of the coatings were evaluated using scanning electron microscopy (SEM) and transmission electron microscopy. Hardness was measured using microhardness tester. Wear test was carried out with the help of 'Bruker' tribometer. Worn surfaces were characterised employing SEM. Results show that TiCrN coating has crystalline columnar structure and other coatings have nano-crystalline structures. Besides improved hardness, TiAlN has best wear resistance and TiCrN coating exhibits least friction coefficient.

Keywords: Thin Film; Wear; Friction; Hardness; Microstructure

1. INTRODUCTION

Hybrid bearings are next generation bearings which results in several advantages¹⁻². Significantly reduced weight, significantly increased capabilities to operate at higher temperatures and increased speeds, dramatically increased bearing life even under increasingly challenging operating conditions, reliably withstanding poor lubrication conditions including "oil-off" etc. are some of the important advantages of hybrid bearings³. These bearings are actively serving a range of aerospace segments including helicopters, gearboxes, transmissions, aero-engines, hot air valves, actuation systems, surveillance systems, space mechanisms, rockets. In addition, hybrid bearings may find extensive applications in ramjet and scramjet engines.

Aero-engine of present time is undergoing continuous improvement. Efforts are on to improve not only the efficiency of the engine, but also the speed of the aircraft. This necessarily requires operation of various parts at higher speed. Reduction of engine weight is another necessary prerequisite for such attempt. This has resulted requirement of hybrid bearing where balls or rollers of the bearings are made of ceramic materials such as Si₃N₄ and races and cages are made of metallic parts. However, since a ceramic part is made to rotate or slide against a metallic part in bearing assembly, it is necessary to provide a ceramic protective coating on the metallic parts⁴.

PVD protective layers are applied to ensure protection for industrially used tools against wear. Because of their excellent

wear resistance, Ti-based coating systems, such as TiN, TiCrN, or TiAlN, are extensively used in varieties of industries⁵⁻⁷. The hardness of TiAlN coating varies between 28–32 GPa in addition to its extraordinary tribological properties⁸. Presence of aluminium allows the layer to operate up to 800 °C⁹. A thin, dense and adherent protective alumina layer is formed during sliding and this minimizes diffusion-induced wear^{8,10}. In contrast, TiCrN coating is investigated to a less extent. Protective hard TiCrN coating exhibits superior resistance to wear and corrosion. The TiN and CrN phases of TiCrN oxidize to TiO₂ and Cr₂O₃¹⁰⁻¹². TiN/SiN_x nanocomposite coating is relatively newer version of wear resistance coating. Chemical vapour deposition¹³, reactive magnetron sputtering^{14,15}, are demonstrated process for depositing nanocomposite films. Reactive hybrid processes are established method for the deposition of TiN/SiN_x nanocomposite layers^{16,17}. Systematic study to understand the microstructure and mechanical properties of nc-TiN/ α -SiN and nc-TiCN/ α -SiCN super hard films on c-Si substrate has been reported¹⁸. However, tribological study of these coating and correlation with microstructure is quit scanty. These thin films applied by PVD technique can be considered to be potential layers for protection of metallic parts against ceramic counter-bodies in hybrid bearings system. In view of the above, present investigation has been undertaken to examine the microstructure and wear performance of TiAlN, TiCrN and n-TiAlN/ α -Si₃N₄ coatings deposited by cathodic arc physical vapour deposition (CA-PVD) technique on M-50 steel under dry condition. This technique is chosen because it gives protective hard coatings with higher density and higher adhesion strength than other conventional PVD process.

2. METHODS AND MATERIAL

Three different categories of hard protective coatings namely, TiAlN, TiCrN and *n*-TiAlN/*α*-Si₃N₄ were deposited on M-50 steel substrates using (CA-PVD) technique. M 50 steel was obtained by vacuum induction melting followed by vacuum arc refining. Subsequently this steel was hot forged and annealed to relief stresses. The annealed steel was subsequently preheated to 850 °C and soaked for 30 min. The temperature was then raised from 850 °C to 1110 °C and soaked for five minutes followed by oil quenching. Stress relieving was done at 175 °C for 2 hr/inch thickness followed by quenching and holding for two hours in liquid nitrogen at -73 °C. The material was then tempered twice at 540 °C for 2 hr/inch thickness followed each time by air cooling. This heat treated steel is designated as substrate material. Elemental analysis of the substrate material was done using inductively coupled plasma optical emission spectrophotometer (ICP-OES). Interstitial elements were detected by LECO oxygen, nitrogen analyser.

The schematic representation of cathodic arc, physical vapour deposition (CA-PVD) unit is made in Fig. 1. A cathodic arc is a low-voltage, high-current plasma discharge. The process can be made reactive by introducing a reactive gas, for example, nitrogen, in the argon plasma. The arc current is concentrated at the cathode at discrete sites called cathode spots ~1–10 μm in size. The current carried by a cathode spot reaches 1–10 A. A typical arc discharge current of a few 100 A gives rise to a dense plasma of cathode material. As CA-PVD is a very high-energy process (the arc temperature will be close to 15000 °C) most of the condensing atoms will be in ionic form (60 – 90%) and hence by applying a small bias to the substrate one can achieve maximum adhesion strength. Further, by optimization of deposition parameters like substrate bias, target power, reactive gas, etc., desired microstructure or property can be achieved. A 99.99% pure Ti, Cr and AlSi (Al-82% & Si-18%) cathodes were used for all the depositions. The deposition parameters such as the substrate temperature, bias voltage and reactive gas pressure were maintained constant throughout the process. The deposition time was controlled to achieve 4 μm thick coating. The substrates were thoroughly

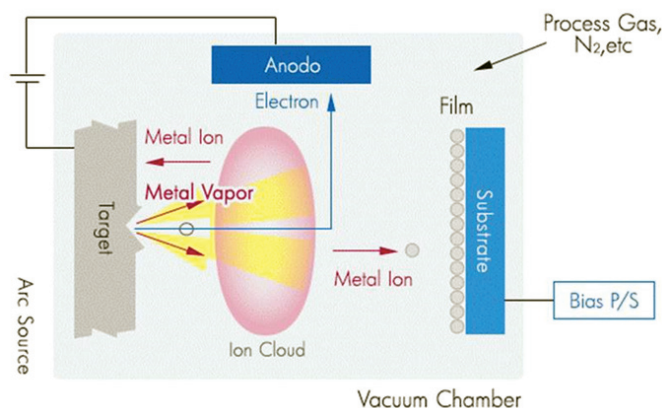


Figure 1. The schematic representation of deposition unit.

cleaned prior to all the depositions using standard procedure involving steps: (i) ultrasonic cleaning, (ii) IR drying and (iii) Ar and metal ion etching. The detail deposition parameters are listed in Table 1. Further detail on the optimisation of coating parameter are available in ref¹⁹⁻²¹.

Table 1. Film deposition conditions

Coating	Substrate Bias (V)	Deposition Pressure (mbar)	Substrate Temperature (°C)	Coating Thickness (μm)	Roughness (nm)
TiAlN	50	5 x 10 ⁻²	450	4	100 ± 15
TiCrN	30	5 x 10 ⁻²	380	3	90 ± 16
<i>n</i> -TiAlN/ <i>α</i> -Si ₃ N ₄	40	5 x 10 ⁻²	450	4	70 ± 10

The composition of the deposited coating was analysed using Cameca make, SX-100 model Electron Probe Micro Analyser (EPMA). Nitrogen concentration was deduced by differential method from the analyzed data. The hardness of the coating was measured by AFFRI (Model no VRSD-279) micro-hardness tester. Since the coatings were brittle in nature, cross section TEM samples were prepared by a dual beam scanning electron microscopy (SEM) equipped with a micro-manipulator, the ‘Omniprobe’. The different stages of sample preparation involved, initial protective platinum deposit, followed by trench digging (regular cross section) and thinning from both sides (cleaning cross section) resulting in formation of a lamella. The created lamella was at first welded to the micromanipulator by platinum deposit, and then separated from the bulk by using the focused ion beam (FIB). The lamella was carefully lifted off and then re-welded to an omniprobe grid, a grid in the form of a half-moon structure that can be directly inserted in the TEM after final thinning of the sample to electron transparency. The samples were analysed in the transmission electron microscopy (FEI make 200kV Tecnai G2 TEM).

Wear test was carried out using a Brucker tribometer under unidirectional sliding motion at ambient condition. The image of the Brucker tribometer is presented in Fig. 2. The schematic of ball on disc configuration used in present study is made in Fig. 3. The diameter of the coated disc was 38 mm. The tribometer is equipped with high performance torque sensor and dual force sensors. The tribometer is interfaced with computer having RS 232 interface for the acquisition of data. Wear tests were performed at loads 0.5 N, 1.0 N, and 2.0 N for sliding velocity of 1 m/s. Si₃N₄ ceramic balls of 6 mm diameter were used as counter body.

Coatings and counter bodies were thoroughly cleaned with ethanol prior to experiments. The sliding tests were performed in ambient air at 23 °C and 65 % relative humidity. The test duration was controlled to have just visible wear scar under an optical microscope after the test. Wear was measured using a non-contact optical profilometer after the end of wear test. The morphologies of the worn samples are examined with the help of SEM to understand the material removal mechanism.



Figure 2. Image of brucker tribometer.

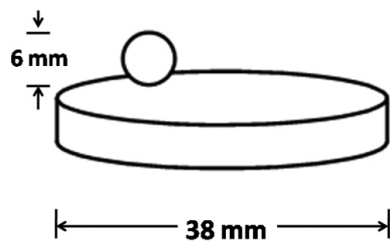


Figure 3. Schematic of ball on disc configuration.

3. RESULTS AND DISCUSSION

3.1 Composition and Microstructures of the Substrate and the Coatings

The optical micrograph of the substrate is provided in Fig. 4. A tempered martensite microstructure is evident. The measured composition of the substrate steel is summarised in Table 2. The steel contains 4.2 % Mo, 4.1 % Cr, about 1 % of V, 0.032 % Ni and around 1 % C.

Table 2. Chemical composition of the substrate materials M-50 steels

C	Mn	Si	Cr	Ni	Mo	V	Cu	S	P
0.7	0.3	0.2	3.7	0.1	4.0	1.0	0.05	0.01	0.01

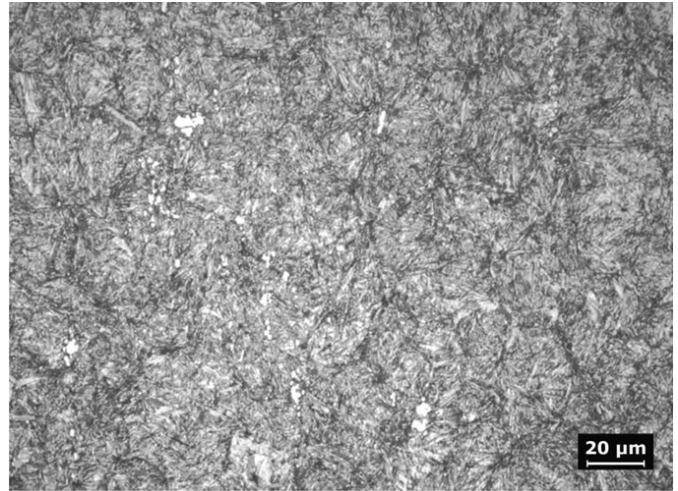


Figure 4. The optical micrograph of M 50 steel.

SEM images showing the morphology of TiAlN, TiCrN and n-TiAlN/ α -Si₃N₄ coatings are presented in Fig. 5. All the coatings show presence of micro-droplets on the coated surface and this feature is common for cathodic arc deposition technique and the coating deposited by this technique exhibits best combination of density and hardness. SEM images showing the transverse section of the coatings are presented in Fig. 6. A defect free coating with smooth interface is evident. Thicknesses of TiAlN, TiCrN and n-TiAlN- α -Si₃N₄ coatings are 4 μ m, 3 μ m, and 4 μ m, respectively. The composition of the coating obtained by electron probe micro analyser (EPMA) is listed in Table 3. The n-TiAlN/ α -Si₃N₄ coating contains the highest amount of Ti. Coatings TiAlN and TiCrN exhibit the maximum and the minimum amount of N respectively.

The low magnification TEM images of the coatings are presented in Fig. 7. Layered structure of n-TiAlN/ α -Si₃N₄ coating is apparent and such structure is due to growth interruption. The microstructure of TiAlN coating revealed a nano granular structure. There are areas with nano grains having coarse and fine structures. A crystalline columnar microstructure can be seen for TiCrN coating. The high magnification TEM images and the corresponding diffraction patterns obtained from the coatings are illustrated in Fig. 8. The TEM image and the diffraction rings of n-TiAlN/ α -Si₃N₄ coating confirm nano structure. The high magnification TEM

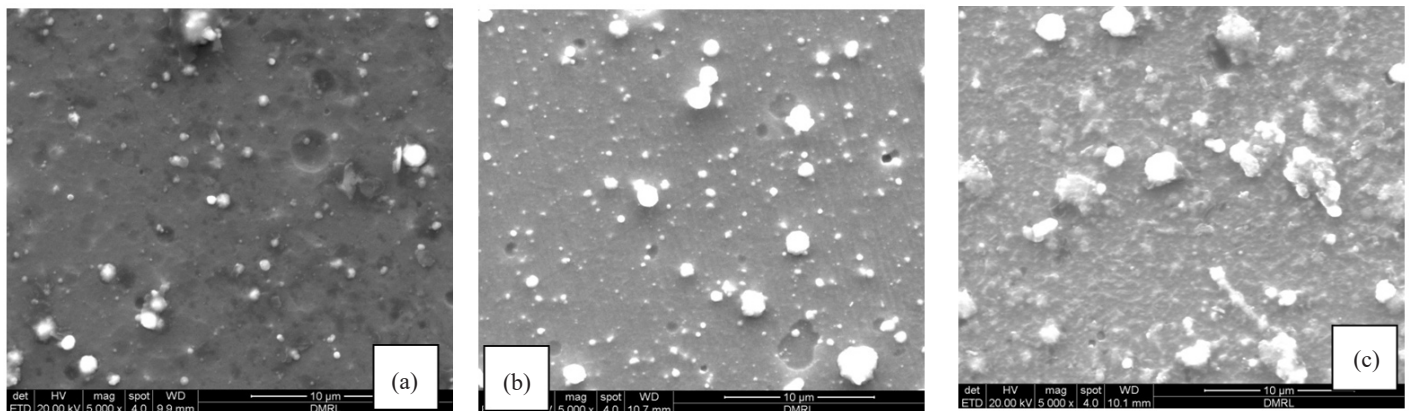


Figure 5. SEM images showing the morphology of (a) TiAlN, (b) TiCrN and (c) n-TiAlN/ α -Si₃N₄ coatings.

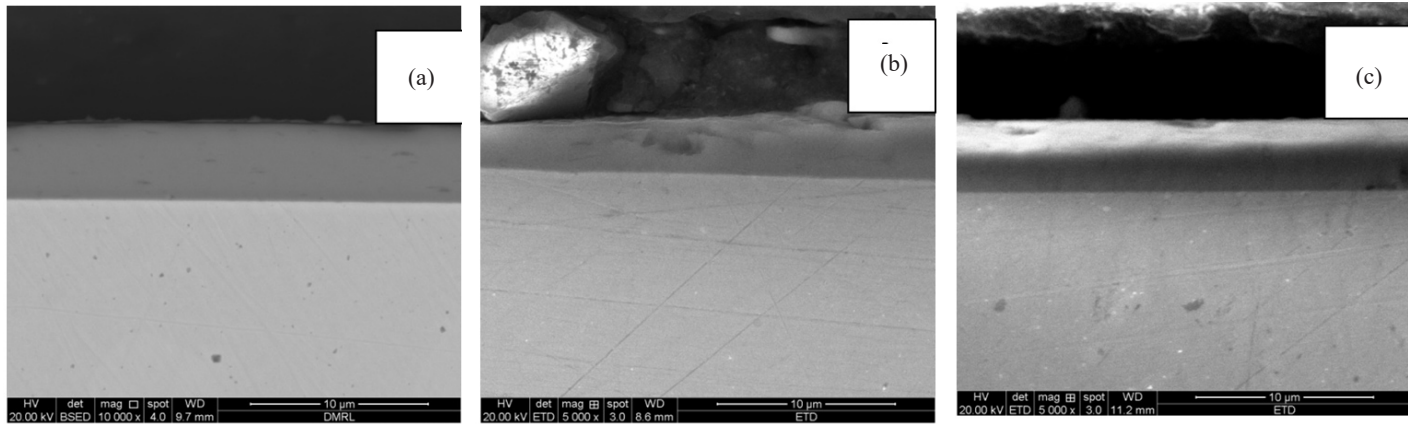


Figure 6. SEM images showing the transverse section of (a) TiAlN, (b) TiCrN and (c) n-TiAlN/ α -Si₃N₄ coatings.

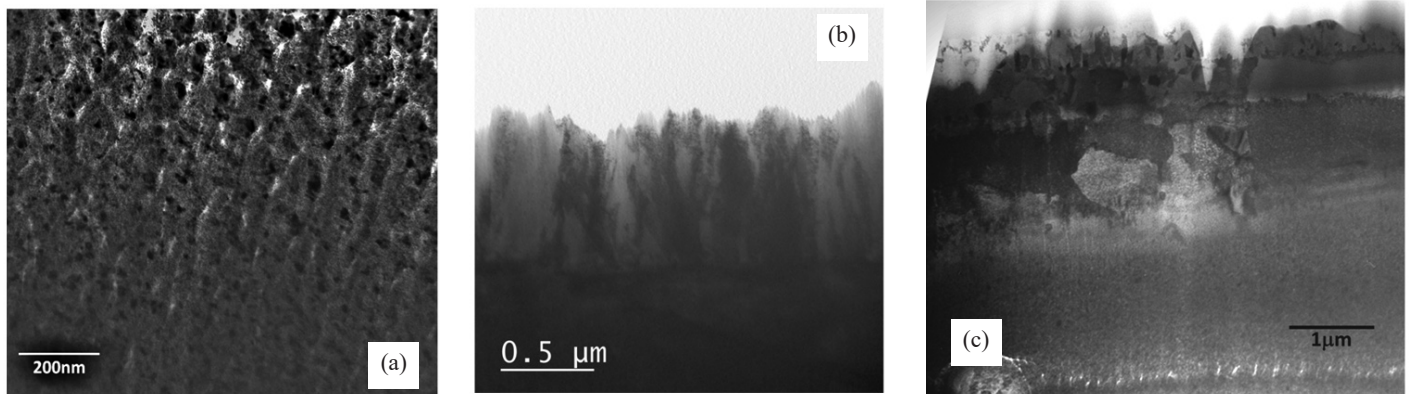


Figure 7. Low magnification TEM image of (a) TiAlN, (b) TiCrN and (c) n-TiAlN/ α -Si₃N₄ coating.

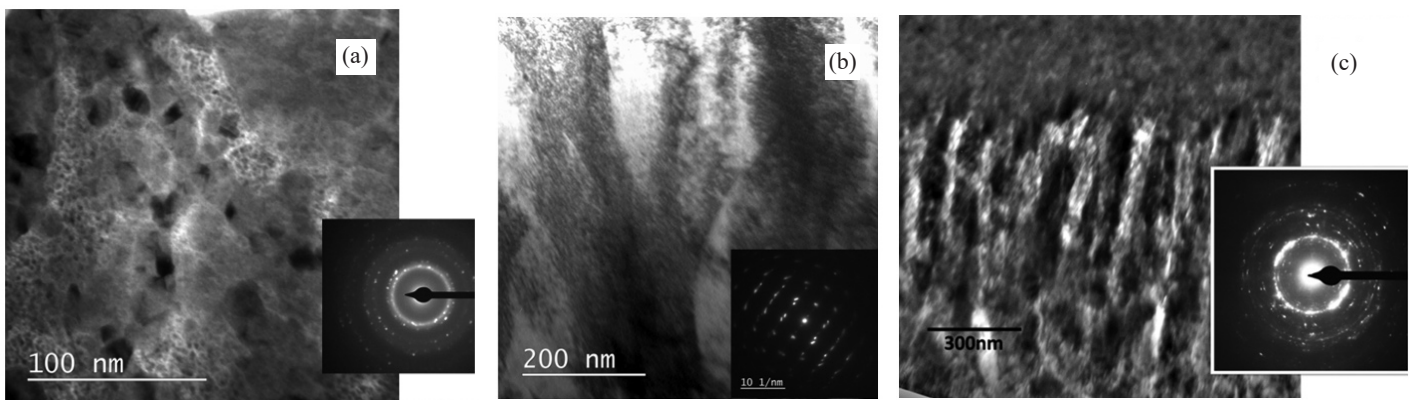


Figure 8. High magnification TEM image of (a) TiAlN, (b) TiCrN and (c) n-TiAlN/ α -Si₃N₄ coating.

Table 3. Composition of the films as measured by EPMA

Coating	Ti (wt %)	Al (wt %)	Cr (wt %)	Si (wt %)	N (wt %)
TiAlN	33.0 ± 1.2	38.5 ± 1.5	-	-	28.5 ± 1.2
TiCrN	39.4 ± 1.5	-	40.9 ± 2.0	-	19.7 ± 0.9
n-TiAlN/ α -Si ₃ N ₄	47.6 ± 2.0	20.2 ± 1.0	-	4.4 ± 2.1	27.8 ± 1.4

image with corresponding ring pattern formation during selected area diffraction (SAD) of TiAlN coating reaffirm nano crystalline structure. The high magnification TEM image along with corresponding diffraction pattern of TiCrN coating confirms coarse grain.

3.4 Mechanical Properties of the Coatings

High roughness of films deposited by this technique makes it difficult to carryout nano-hardness measurement or to report data on elastic modulus using nano-indenter. The hardness of the coatings as measured by micro-indenter is given in the form of bar diagram in Fig. 9 along with the hardness of the substrate material. At the given applied load and for the given hardness of the coatings, the depth of deformation goes beyond the coating and the hardness value is affected by hardness of the substrate material. However, for all coatings substrate material remains same. Thus, it can be assumed safely that relative values of the

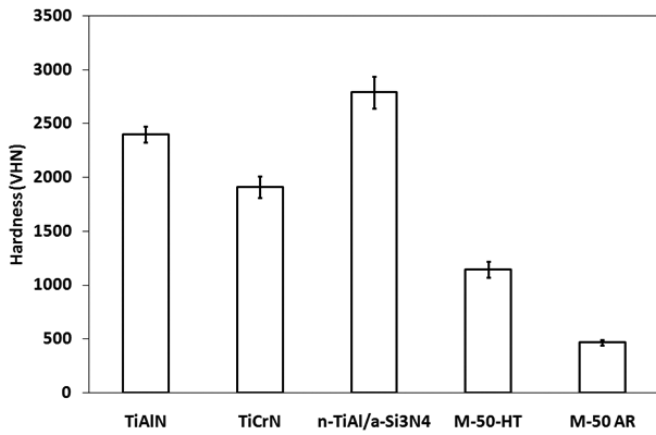


Figure 9. The hardness of the investigated coatings.

hardness of the coatings remain unchanged. It is clear from Fig. 9 that hardness of all coatings is higher than the hardness of the substrate material. Among various coatings, n-TiAlN/α-Si₃N₄ nanocomposite coating has exhibited the highest hardness followed by TiAlN coating. The highest hardness is due to dispersion strengthening because of presence of α-Si₃N₄ in TiAlN matrix.

3.5 Wear Behaviour

The variation of friction coefficient of the coated steels against Si₃N₄ balls at an applied load of 1.0 N as function of time is presented in Fig. 10. The friction coefficient reaches a steady state value after an initial run in period for all coatings and the substrate material. The steady state friction coefficients of TiAlN and n-TiAlN/α-Si₃N₄ composite coating are comparable and are around 0.8. In contrast, TiCrN coating exhibits significantly lower steady state friction coefficient which is around 0.6. The friction coefficient of TiCrN coating is low due to lubricious properties of Cr₂O₃ scale²² that forms during sliding¹⁰. The friction coefficient of the substrate is in between these two values. The variation of friction coefficient of n-TiAlN/α-Si₃N₄ composite coating as function of time at three different loads is given in Fig. 11. After a run in period, steady state friction coefficient is reached at applied load of 1.0 N and 2.0 N. However, at applied load of 0.5 N, the friction coefficient increases continuously even after the run

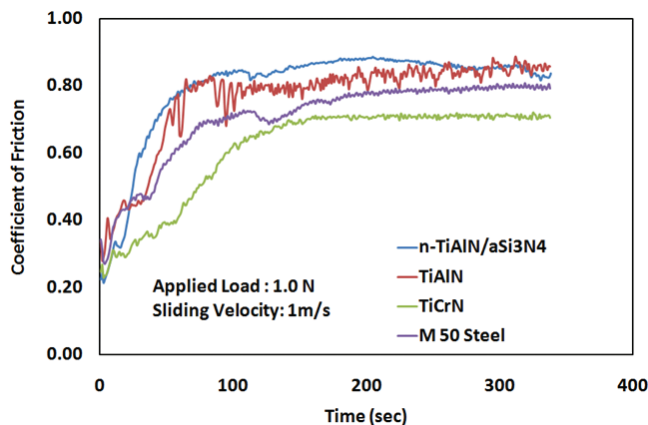


Figure 10. Variation of friction coefficient with time for all coatings at 1.0 N applied load.

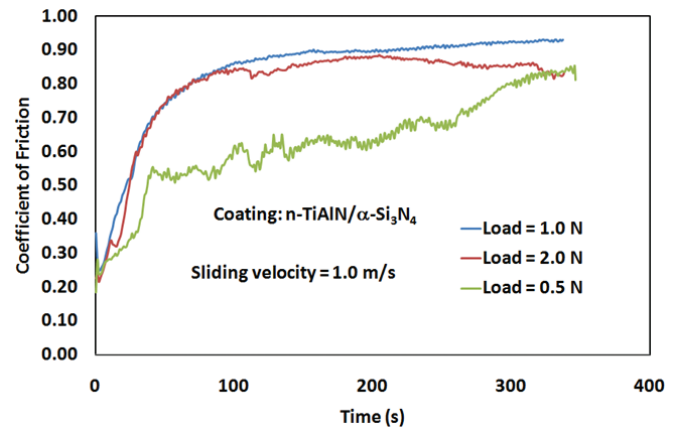


Figure 11. Variation of friction coefficient with time for n-TiAlN/α-Si₃N₄ coatings at different applied load at sliding velocity of 1 m/s.

in period. The steady state friction coefficient is nearly 0.8 irrespective of the applied load. The load independence of the friction coefficient is indication of the fact that adhesion does not govern friction²³. Although, friction coefficient is high in dry sliding condition, it will be significantly low under lubrication condition especially under elastohydrodynamic or hydrodynamic lubrication condition which is expected to be the prevailing condition.

The total wear as measured using a non-contact optical profilometer after the end of wear test at an applied load of 1.0 N is provided in the form of bar diagram in Fig. 12. All coatings exhibit lower wear rate compared to the substrate. Among these coatings wear rate is the minimum for TiAlN coating. The reason for this is formation of Al₂O₃ scale which has very high hardness²⁴. Scale forms because of high flash temperature generated at the contact point¹⁰. Thus, it can be stated that all coating are promising coating for application requiring wear resistance. There will be no catastrophic wear of the parts even if the system operates under boundary or mixed lubrication regime.

The morphologies of the worn surfaces are presented in Fig. 13. Extensive plastic deformation under multiaxial compressive load is the main features of the worn surfaces. Although, delamination crack can be seen on the worn surface

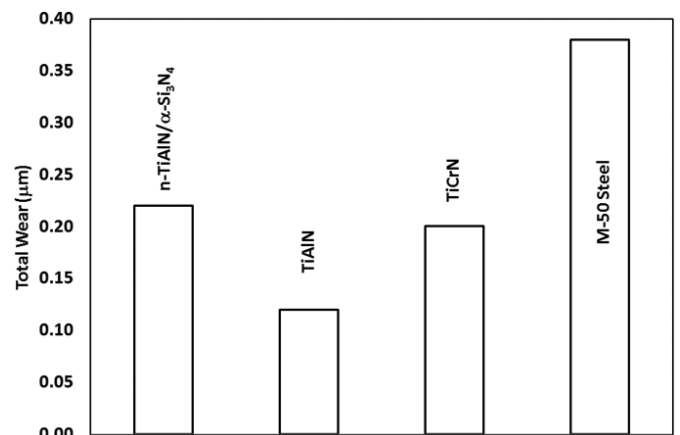


Figure 12. Bar diagram showing the total wear of various coatings and substrate material.

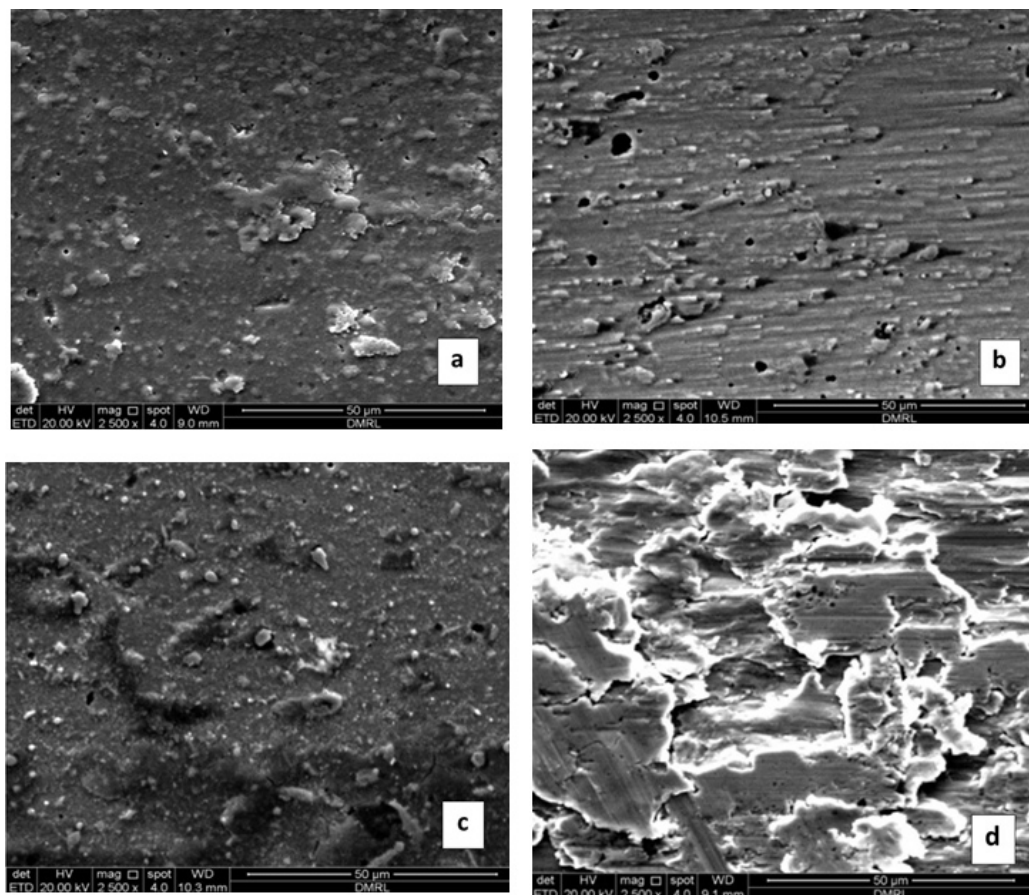


Figure 13. SEM images showing the morphology of the worn surfaces of various coatings and substrate material. (a) TiAlN, (b) TiCrN, (c) n-TiAlN/ α -Si₃N₄ coating and (d) M-50 steel.

of substrate materials, such features are absent on the worn surfaces of the coatings. Further, presence of shear dimples on the worn surface of substrate material indicates significant plasticity. In contrast, the coating materials are removed primarily by brittle chipping. Composition obtained from the worn surfaces by EDS analysis is summarised in Table 4. Quantitative analysis also indicates composition similar to the original coating. This indicates the fact that there is no transfer of materials from the counter-body and also minimum oxidation of the coated surface during sliding.

At this stage it is pertinent to discuss relevance of microstructure of each coating on their wear properties. These coating were deposited after optimizing the processing conditions to get best combination of mechanical properties for each varieties of coatings by previous work¹⁹⁻²¹. It is also to be stated that best combination of mechanical properties need not necessarily provide best wear properties. Thus, there is surely extended research possible on optimization of microstructure for best wear properties for each variety of films and this constitute our future research.

4. CONCLUSIONS

Thin hard coatings of TiAlN, TiCrN and n-TiAlN/ α -Si₃N₄ are deposited using cathodic arc physical vapour deposition technique. The main conclusions of this investigation are listed below

Table 4. Composition of the films as measured by EDS after wear

Coating	Ti (wt %)	Al (wt %)	Cr (wt %)	Si (wt %)	N (wt %)
TiAlN	32.0 ± 3.0	41.2 ± 4.5	-	-	26.8 ± 3.1
TiCrN	38.3 ± 4.0	-	38.8 ± 4.0	-	22.3 ± 3.2
n-TiAlN/ α -Si ₃ N ₄	50.2 ± 6.0	19.3 ± 2.5	-	4.7 ± 4.8	25.8 ± 3.4

- (i) TiAlN and n-TiAlN/ α -Si₃N₄ coatings have nano-crystalline structures. TiCrN coating has crystalline columnar structure.
- (ii) Hardness of the coatings is very high. n-TiAlN/ α -Si₃N₄ coating exhibits the highest hardness followed by TiAlN coating.
- (iii) Friction coefficient under dry sliding condition is quite high. TiCrN coating exhibits least friction coefficient at an applied load of 1.0 kg.
- (iv) All coatings exhibit improved wear resistance. TiAlN has the highest wear resistance.

ACKNOWLEDGEMENT

Authors are grateful to Director, DMRL for granting permission to publish this work. Authors acknowledge the constructive reviews of some reviewers.

REFERENCES

1. Lu, D.; Zhao, W.; Lu, B. & Zhang, J. Static characteristics of a new hydrodynamic–rolling hybrid bearing. *Tribology International*, 2012, **48**, 87-92.
doi: 10.1016/j.triboint.2011.11.010
2. Sharma, S.C.; Phalle, V.M. & Jain, S.C. Influence of wear on the performance of a multirecess conical hybrid journal bearing compensated with orifice restrictor. *Tribology International*, 2011, **44** (12), 1754-1764.
doi: 10.1016/j.triboint.2011.06.032
3. Tian Y. & Bonis M. Analytical approach for the determination of the dynamic coefficients of hybrid bearings. *Wear*, 1995, **188** (1-2), 66-76.
doi: 10.1016/0043-1648(95)06615-2
4. Zhang, G.; Yuun, X. & Dong, G. The tribological behavior of Ni–Cu–Ag-based PVD coatings for hybrid bearings under different lubrication conditions. *Tribology International*, 2010, **43**, 197-201.
doi: 10.1016/j.triboint.2009.05.032
5. Navinšek, B. & Žabkar, A. Improvement of cold forming and form cutting tools by PVD TiN coating. *Vacuum*, 1986, **36** (1-3), 111–115.
doi: 10.1016/0042-207X(86)90282-4
6. Kavasnica, S.; Schalko, J.; Eisenmenger-Sittner, C.; Bernardi, J.; Vorlaufer, G., Pauschitz, A. & Roy, M. Nanotribological study of PECVD DLC and reactively sputtered Ti containing carbon films. *Diam. Relat. Mater.*, 2006, **15**, 1743.
7. Jehn, H. A. Multicomponent and multiphase hard coatings for tribological applications. *Surf. Coat. Tech.*, 2000, **131**, 433–440.
doi: 10.1016/S0257-8972(00)00783-0
8. PalDey, S. & Deevi, S. C. Single layer and multilayer wear resistant coatings of (Ti,Al)N: A review. *Mat. Sci. Eng. A-Struct.*, 2003, **A 342** (1-2), 58–79.
9. Kawate, M.; Kimura Hashimoto, A. & Suzuki, T. Oxidation resistance of Cr1–XAlXN and Ti1–XAlXN films. *Surf. Coat. Tech.*, 2003, **165** (2), 163–167.
doi: 10.1016/S0257-8972(02)00473-5
10. Roy, M. Using of Wear mechanism maps to engineer surfaces for enhanced wear resistance. *T. Ind. Inst. Met.*, 2009, **62**, 197-208.
doi: 10.1007/s12666-009-0032-y
11. Roy, M.; Ray, K.K. & Sundararajan, G. The influence of erosion-induced roughness on the oxidation kinetics of Ni and Ni-20Cr alloy. *Oxid. Met.*, 1999, **51**, 251-272.
doi: 10.1023/A:1018870606617
12. Vepr'ek, S. & Reiprich, S. A concept for the design of novel superhard coatings. *Thin Solid Films*, 1995, **268**, 64-71.
doi: 10.1016/0040-6090(95)06695-0
13. Pauschitz, A.; Schalko, J.; Koch, T.; Eisenmenger-Sittner, C.; Kavasnica, S. & Roy, M. Nanoindentation and AFM study of PECVD DLC and reactively sputtered Ti containing carbon films. *Bull. Mater. Sci.*, 2003, **26**, 585-591.
doi: 10.1007/BF02704320
14. Diserens, M.; Patscheider, J. & Levy, F. Mechanical properties and oxidation resistance of nanocomposite TiN–SiN_x physical-vapor-deposited thin films. *Surf. Coat. Tech.*, 1999, **120–121**, 158-165.
doi: 10.1016/S0257-8972(99)00481-8
15. Tomala, A.; Roy, M. & Franek, F. Nanotribology of Mo–Se–C films. *Philosophical Magazine*, 2010, **90** (29), 3827-3843.
doi: 10.1080/14786435.2010.495041
16. Pauschitz, A.; Badisch, E.; Roy, M. & Shtansky, D.V. On the scratch behaviour of self lubricating WSe₂ film. *Wear*, 2009, **267**(11), 1909-1914.
doi: 10.1016/j.wear.2009.03.037
17. Diserens, M.; Patscheider, J. & Levy, F. Improving the properties of titanium nitride by incorporation of silicon. *Surf. Coat. Tech.*, 1998, **108–109**, 241.
doi: 10.1016/S0257-8972(98)00560-X
18. Jedrzejowski, P.; Klemberg-Sapieha, J.E. & Martinu, L. Quaternary hard nanocomposite TiC_xN_y/SiCN coatings prepared by plasma enhanced chemical vapor deposition. *Thin Solid Films*, 2004, **466** (1–2), 189-196.
doi: 10.1016/j.tsf.2004.03.043
19. Pemmasani, S.P.; Valleti, K.; Rama Krishna, M.; Rajulapati, K.V.; Gundakaram, R.C. & Joshi, S.V. Structure property correlation in cathodic arc deposited TiAlN coatings. *Mater. Sci. Forum.*, 2012, **701–703**, 967-970.
doi:10.4028/www.scientific.net/MSF.702-703.967
20. Valleti, K.; Puneet, C; Rama Krishna, L. & Joshi, S.V. Studies on cathodic arc PVD grown TiCrN based erosion resistant thin films. *J. Vac. Sci. Technol. A.*, 2016, **A34** (4) 041512-1to 041512-7.
doi: 10.1116/1.4953466
21. Ravi, N., Markendya, R. & Joshi, S.V. Effect of substrate roughness on adhesion and tribological properties of nc-TiAlN/ α -Si₃N₄ nanocomposite coatings deposited by cathodic arc PVD process. *Surface Engineering*, 2017, **33** (1), 7-19.
doi: 10.1179/1743294415Y.0000000005
22. Sert, Y. & Toplan, N., Tribological behaviour of a plasma sprayed Al₂O₃-TiO₂-Cr₂O₃ coating. *Mater. Technol.*, 2013, **47** (2), 181-183.
23. Roy, M.; Koch, T. & Pauschitz, A. Influence of sputtering procedure on the indentation and scratch behaviour of WS₂ film. *Appl. Surf. Sci.*, 2010, **256**, 6850-6858.
doi: 10.1016/j.apsusc.2010.04.100
24. Brums, C. & Schutze, M. Investigation of the mechanical properties of oxide scales on nickel and TiAl. *Oxid. Met.*, 2001, **55** (1-2), 35-68.
doi: 10.1023/A:1010321108212

CONTRIBUTORS

Dr Manish Roy graduated from Indian Institute of Technology, Kharagpur in 1985 in Metallurgical Engineering. After a short stay with an integrated steel plant as ‘Junior Manager’ he joined for his post graduation study. Following post graduation he joined ‘Defence Metallurgical Research Laboratory’ in 1989 as scientist. His areas of research interest are materials and surface engineering for tribological application and nanotribology of

self lubricating films. He is particularly interested in various interactions between oxidation and tribology and also between corrosion and tribology. He has around 100 papers in various reviewed national and international journals. He is edited two books on 'Surface Engineering for Enhanced Performance against Wear' (Springer) and 'Thermal Sprayed Coatings and Their Tribological Performances' (IGI Global).

Mr Sabyasachi Saha, completed BSc Physics (honours) from St. Stephens College, University of Delhi in the year 2003. He did MSc in Physics from Indian Institute of Technology, Delhi in the year 2005. Then he completed MTech in Optoelectronics and Optical Communication from Indian Institute of Technology, Delhi in the year 2007. After that he has been working as a Scientist in the Electron Microscopy Group at Defence Metallurgical Research Laboratory, Hyderabad. His research interests include electron microscopy and sample preparation

using the Dual Beam SEM. He is currently also involved in characterization of various semiconductor materials especially GaN based heterostructures and also wide band gap SiC. Contribution in the current study he was responsible for carrying out TEM investigation.

Dr Krishna Valleti is a researcher working as a senior scientist at International Advanced Research Centre for Powder Metallurgy and New Materials (ARCI). He has received his PhD in Physics in the area of thin films from Indian Institute of Technology (IIT), Madras. His major research interests include thin films science, in particular, developing and understanding of variety of Physical Vapor Deposited (PVD) thin films in different configurations for different applications (cutting tools, dies, compressor blades, solar thermal receiver tubes, etc.) In the current study he was involved in depositing the films investigated.